

# ALIEN EARTHS

## EARTHS IN OTHER SOLAR SYSTEMS

### Recent Publications

*Bayesian analysis of Enceladus's plume data to assess methanogenesis*

*Hydration of Nebular Minerals through the Implantation-Diffusion Process*

*The Mass Budgets and Spatial Scales of Exoplanet Systems and Protoplanetary Disks*

*Atomic-scale Evidence for Open-system Thermodynamics in the Early Solar Nebula*

*Redox Hysteresis of Super-Earth Exoplanets from Magma Ocean Circulation*

*LBT Reveals Large Dust Particles and a High Mass-loss Rate for K2-22 b*

*Imaging low-mass planets within the habitable zones of nearby stars with ground-based mid-infrared imaging*

*A large sub-Neptune transiting the thick-disk M4V TOI-2406*

*ACCESS and LRG-BEASTS: A Precise New Optical Transmission Spectrum of the Ultrahot Jupiter WASP-103b*

*EDEN: Flare Activity of the Nearby Exoplanet-hosting M Dwarf Wolf 359 Based on K2 and EDEN Light Curves*

*Bioverse: A Simulation Framework to Assess the Statistical Power of Future Biosignature Surveys*



**Earths in Other Solar Systems** and Alien Earths are part of NASA's Nexus for Exoplanetary System Science program, which carries out coordinated research toward the goal of searching for and determining the frequency of habitable extrasolar planets with atmospheric biosignatures in the Solar neighborhood.

Our interdisciplinary teams includes astrophysicists, planetary scientists, cosmochemists, material scientists, chemists, biologists, and physicists.

The Principal Investigator of Project EOS and Alien Earths is Daniel Apai (University of Arizona). The projects' lead institutions are The University of Arizona's Steward Observatory and Lunar and Planetary Laboratory.

For a complete list of publications, please visit the [EOS Library](#) and [AE Library](#) on the SAO/NASA Astrophysics Data System.



## Origins Seminar

The **Origins Seminar** series brings together ISM, star and planet formation people, exoplanets experts, planetary scientists and astrobiologists. Topics range from molecular clouds through star and planet formation to exoplanets detection and characterization and astrobiology.

The seminar series is organized by Serena Kim (SO), Kamber Schwarz (LPL), Sebastiaan Krijt (University of Exeter, UK) and Sebastiaan Haffert (SO) from Steward Observatory/Dept. of Astronomy and Dept. of Planetary Sciences (LPL) at the University of Arizona. The Origins Seminar series is partly supported by the Earths in Other Solar Systems NExSS team.

Talks take place **12:00 - 1:00pm (MST) on Mondays**. To receive weekly updates and advertisements for talks, please subscribe to the [mailing list](#). If you are interested in presenting your work during one of the open slots, feel free to contact [the organizers](#).

**Currently, the Origins seminar meets via Zoom due to the Covid-19 Pandemic.** We may continue to meet via zoom through Fall2021, depending on the status of the Pandemic and guidelines by the department and the University. The Zoom information is sent via email.

[Origins Seminars YouTube Channel](#)

# Bayesian analysis of Enceladus's plume data to assess methanogenesis

Antonin Affholder, François Guyot, Boris Sauterey, Régis Ferrière & Stéphane Mazevet

➔ [Nature Astronomy, Volume 5, June 2021](#)

Observations from NASA's Cassini spacecraft established that Saturn's moon Enceladus has an internal liquid ocean. Analysis of a plume of ocean material ejected into space suggests that alkaline hydrothermal vents are present on Enceladus's seafloor. On Earth, such deep-sea vents harbour microbial ecosystems rich in methanogenic archaea. Here we use a Bayesian statistical approach to quantify the probability that methanogenesis (biotic methane production) might explain the escape rates of molecular hydrogen and methane in Enceladus's plume, as measured by Cassini instruments. We find that the observed escape rates (1) cannot be explained solely by the abiotic alteration of the rocky core by serpentinization; (2) are compatible with the hypothesis of habitable conditions for methanogens; and (3) score the highest likelihood under the hypothesis of methanogenesis, assuming that the probability of life emerging is high enough. If the probability of life emerging on Enceladus is low, the Cassini measurements are consistent with habitable yet uninhabited hydrothermal vents and point to unknown sources of methane (for example, primordial methane) awaiting discovery by future missions.

[UArizona Press Release](#)  
[Nature Astronomy News and Views](#)

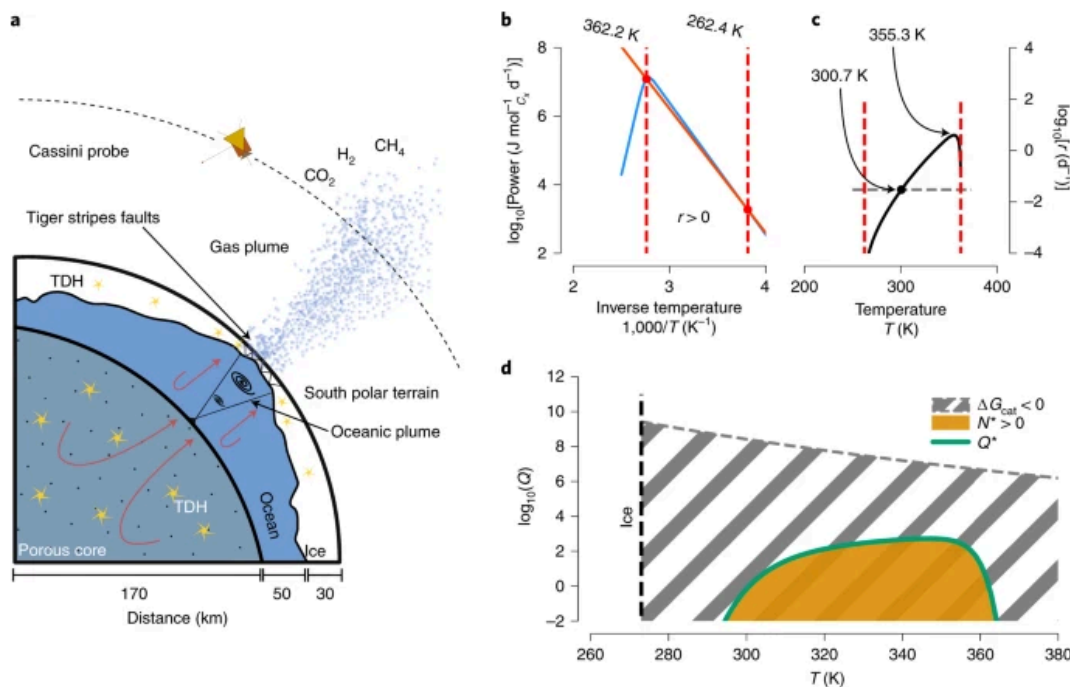


Figure 1: General modelling framework

## Hydration of Nebular Minerals through the Implantation-Diffusion Process

Ziliang Jin, and Maitrayee Bose

→ [The Astrophysical Journal, Volume 913, Number 2](#)

Recent studies have detected structurally bound water in the refractory silicate minerals present in ordinary and enstatite chondrite meteorites. The mechanism for the incorporation of the hydrogen is not well defined. In this paper we quantitatively examine a two-fold process involving the implantation and diffusion of nebular hydrogen ions that is responsible for the hydration of the chondritic minerals. Our simulations show that depending on critical parameters, including the flux of the protons in nebular plasma, retention coefficient, temperature of the silicate minerals, and desorption rate of implanted hydrogen, the implantation of low-energy hydrogen ions can

result in equivalent water contents of ~0.1 wt% in chondritic silicates within 10 years. Thus, this novel mechanism operating in the nebula at  $10^{-3}$  bar pressure and  $<650$  K temperatures can efficiently hydrate the free-floating chondritic minerals prior to the rapid formation of planetesimals inside the snow line, and agree well with the wet accretion scenario for the inner solar system objects.

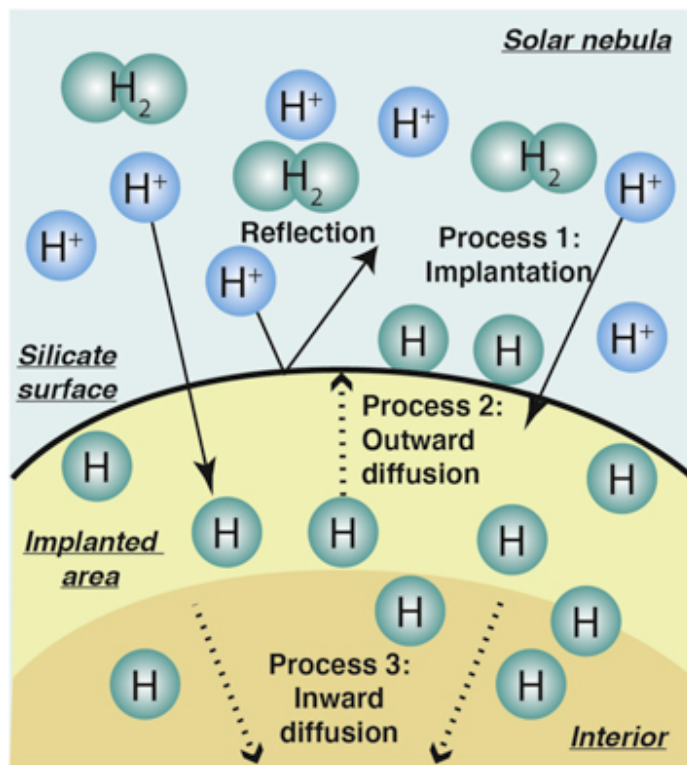


**Figure 1.** A schematic showing the proton implantation–diffusion processes. Ionized  $H^+$  ions in the solar nebular gas are implanted into the top area ( $\leq 100$  nm) of the target silicate grain (Process 1). A fraction of the ionized hydrogen is never implanted but is backscattered to the nebular gas. Due to a concentration gradient in the implanted area of the silicate grain, a portion of the hydrogen recombines with other hydrogen atoms, diffuses outward, and desorbs from the surface of the target (Process 2). The inward diffusion of the rest of the projectile hydrogen leads to a homogeneous distribution of hydrogen in the silicate grain (Process 3).

## The Mass Budgets and Spatial Scales of Exoplanet Systems and Protoplanetary Disks

Mulders, Gijs D. ; Pascucci, Ilaria ; Ciesla, Fred J. ; Fernandes, Rachel B.

→ [Accepted for publication in The Astrophysical Journal](#)

Planets are born from disks of gas and dust, and observations of protoplanetary disks are used to constrain the initial conditions of planet formation. However, dust mass measurements of Class II disks with ALMA have called into question whether they contain enough solids to build the exoplanets that have been detected to date. In this paper, we calculate the mass and spatial scale of solid material around Sun-like stars probed by transit and radial velocity exoplanet surveys, and compare those to the observed dust masses and sizes of Class II disks in the same stellar mass regime. We show that the apparent mass discrepancy disappears when accounting for observational selection and detection biases. We find a discrepancy only when the planet formation efficiency is below 100%, or if there is a population of undetected exoplanets that significantly contributes to the mass in solids. We identify a positive correlation between the masses of planetary systems and their respective orbital periods, which is consistent with the trend between the masses and the outer radii of Class II dust disks. This implies that, despite a factor 100 difference in spatial scale, the properties of protoplanetary disks seem to be imprinted on the exoplanet population.

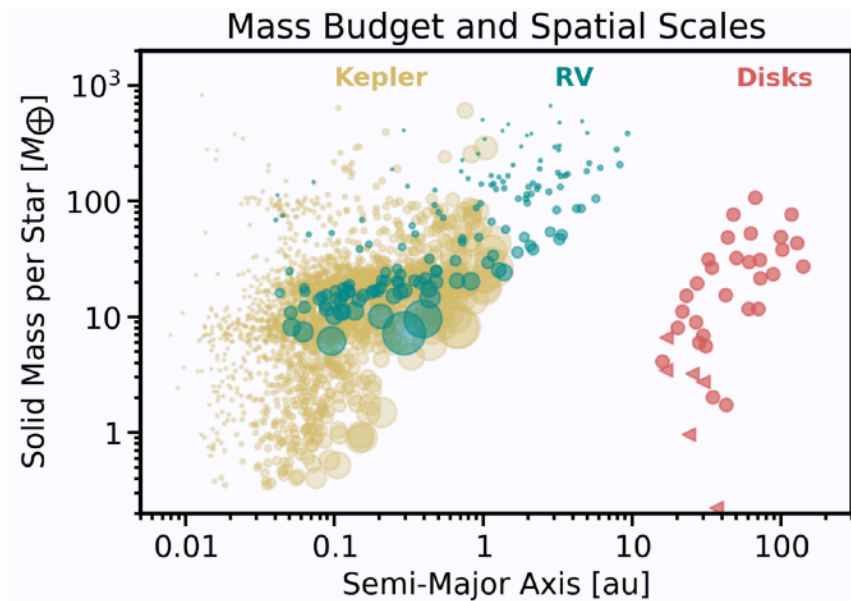


**Figure 7.** Estimated solid system mass vs. spatial scale for exoplanets systems and protoplanetary disks around solar-mass stars. The symbol size is proportional to the inverse survey completeness for each exoplanet to better reflect the true occurrence. The sizes of protoplanetary disks are the radii that enclose 68% of the flux (circles), or an upper limit to that value (triangle).

## Atomic-scale Evidence for Open-system Thermodynamics in the Early Solar Nebula

Zega, Thomas ; Manga, Venkat Rao ; Ciesla, Fred ; Muralidharan, Krishna ; Watanabe, Keitaro ; Inada, Hiromi

### → [The Planetary Science Journal, Volume 2, Issue 3](#)

We report a new integrated framework that combines atomic-length-scale characterization via aberration-corrected scanning transmission electron microscopy with first-principles-driven thermodynamic modeling and dust-transport models to probe the origins of some of the first-formed solids in the solar system. We find that within one of the first solids that formed in our solar system, spinel, nominally  $\text{MgAl}_2\text{O}_4$ , occurs as a twinned inclusion within perovskite,  $\text{CaTiO}_3$ , and contains vanadium segregated to its twin boundary as atomic columns. Our results support a scenario in which spinel condensed at 1435 K in the midplane of the solar protoplanetary disk and was later transported inward to a hotter region where perovskite condensed around it at 1681 K. The spinel became twinned as a result of a displacive phase transition in the perovskite after which it was later transported to cooler regions of the disk and incorporated into its parent asteroid. The condensation, transport, and phase transformation can all be explained within the developed self-consistent framework that reproduces the observed phase assemblage and atomic-scale structure.

This framework suggests that planetary materials evolved within a thermodynamically open system and, moving forward, motivates such an approach in order to understand the thermodynamic landscape on which planetary materials formed.

[UArizona Press Release](#)

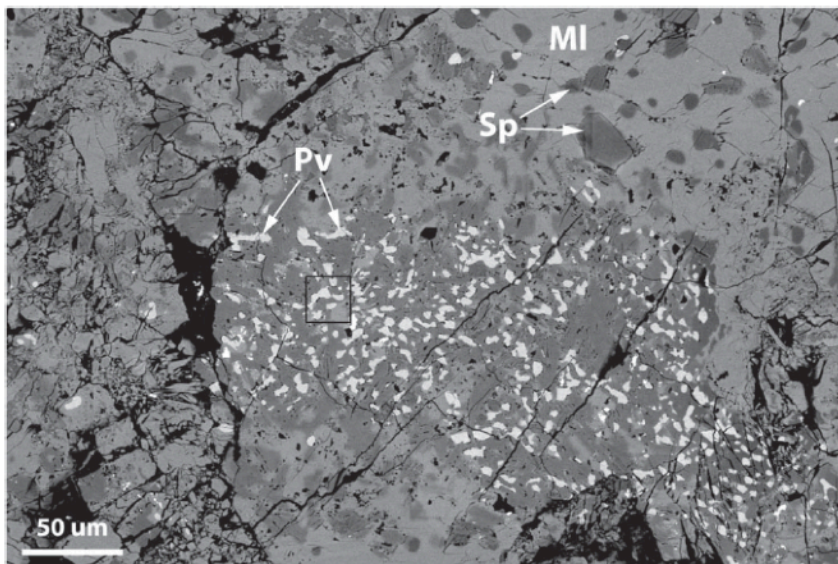


**Figure 1.** Backscatter electron image of a local part of the fluffy type-A CAI in Allende TS25. Melilite (MI) is the most abundant phase in the core of the inclusion and occurs with spinel (Sp) and perovskite (Pv). The black rectangle outlines the area from which FIB section “b” was extracted.

## Redox Hysteresis of Super-Earth Exoplanets from Magma Ocean Circulation

Tim Lichtenberg

→ The Astrophysical Journal Letters, Volume 914, Issue 1

Internal redox reactions may irreversibly alter the mantle composition and volatile inventory of terrestrial and super-Earth exoplanets and affect the prospects for atmospheric observations. The global efficacy of these mechanisms, however, hinges on the transfer of reduced iron from the molten silicate mantle to the metal core. Scaling analysis indicates that turbulent diffusion in the internal magma oceans of sub-Neptunes can kinetically entrain liquid iron droplets and quench core formation. This suggests that the chemical equilibration between core, mantle, and atmosphere may be energetically limited by convective overturn in the magma flow. Hence,

molten super-Earths possibly retain a compositional memory of their accretion path. Redox control by magma ocean circulation is positively correlated with planetary heat flow, internal gravity, and planet size. The presence and speciation of remnant atmospheres, surface mineralogy, and core mass fraction of primary envelope-stripped exoplanets may thus constrain magma ocean dynamics.

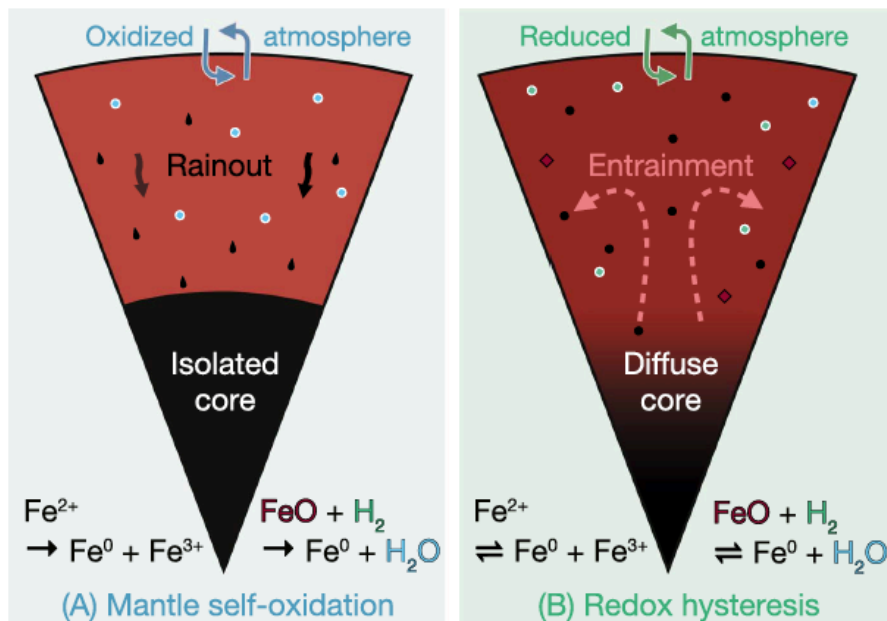


**Figure 2.** Illustration of the two possible end-member cases of magma ocean circulation with varying efficacy of redox reactions that drive changes in primordial mantle composition. (A) Magma ocean circulation is sufficiently vigorous to equilibrate magma and overlying atmosphere, but not energetic enough to entrain liquid iron droplets. These rain out onto the metal core, which results in net oxidation of the mantle via iron disproportionation at high pressure and may sustain endogenic production of water. Secondary atmospheres generated by outgassing from such planetary mantles would be dominated by oxidized species, such as  $H_2O$ ,  $CO_2$ , or  $SO_2$ . (B) In the rainout quenched regime magma circulation is highly turbulent such that the kinetic energy of the large-scale flow entrains liquid iron droplets. This regime may preserve the mantle composition inherited from accretion, diffuse the physical differentiation between silicate mantle and metal core, and result in secondary atmospheres dominated by reduced species, such as  $H_2$ ,  $CO$ , or  $CH_4$ , and their photochemical derivatives.

[Summary Video](#) | [Blog Post](#)

## LBT Reveals Large Dust Particles and a High Mass-loss Rate for K2-22 b

Schlawin, Everett ; Su, Kate Y. L. ; Herter, Terry ; Ridden-Harper, Andrew ; Apai, Dániel

→ The Astronomical Journal, Volume 162, Issue 2

The disintegrating planet candidate K2-22 b shows periodic and stochastic transits best explained by an escaping debris cloud. However, the mechanism that creates the debris cloud is unknown. The grain size of the debris as well as its sublimation rate can be helpful in understanding the environment that disintegrates the planet. Here, we present simultaneous photometry with the  $g$  band at  $0.48 \mu\text{m}$  and  $K_S$  band at  $2.1 \mu\text{m}$  using the Large Binocular Telescope. During an event with very low dust activity, we put a new upper limit on the size of the planet of  $0.71 R_{\oplus}$  or  $4500 \text{ km}$ . We also detected a medium depth transit that can be used to constrain the dust particle sizes. We find that the median particle size must be larger than about  $0.5\text{-}1.0 \mu\text{m}$ , depending on the composition of the debris. This leads to a high mass-loss rate of about  $3 \times 10^8 \text{ kg s}^{-1}$ , which is consistent with hydrodynamic escape models. If they are produced by some alternate mechanism such as explosive volcanism, it would require extraordinary geological activity. Combining our upper limits on the planet size with the high mass-loss rate, we find a lifetime of the planet of less than  $370 \text{ Myr}$ . This drops to just  $21 \text{ Myr}$  when adopting the  $0.02 M_{\oplus}$  mass predicted from hydrodynamical models.

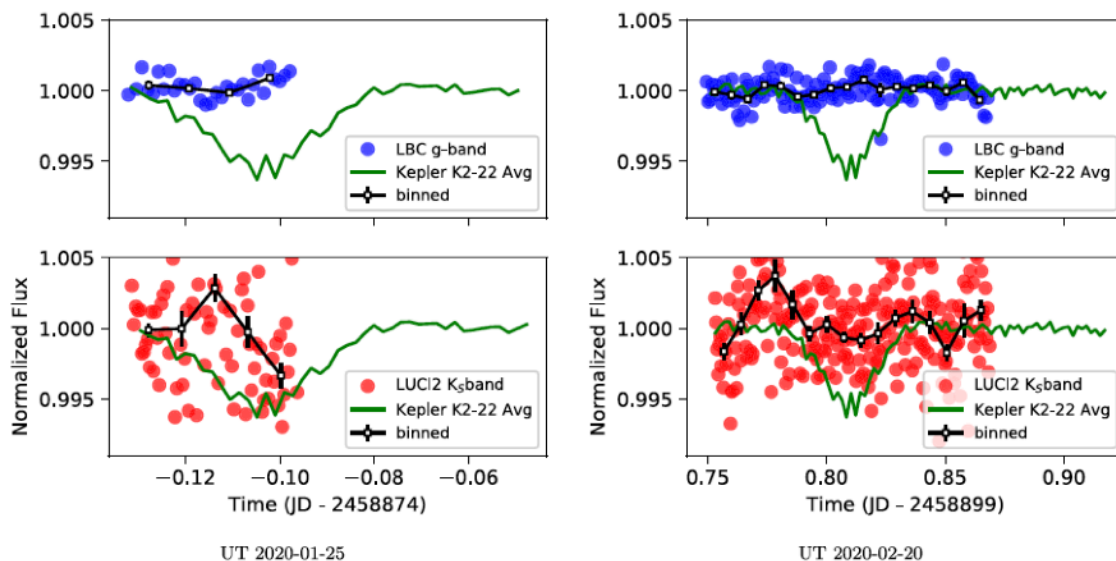


**Figure 1.** Photometry from UT 2020 January 25 and UT 2020 February 20 where transit depths were shallower than the K2 82 days average. The raw photometry is shown as blue and red points for the  $g$  band and  $K_S$  band, respectively, with the binned data as white squares with black error bars. The average phase-folded K2 light curve is shown as a green line. The photometry from UT 2020 February 20 (right) is used to constrain the size of the planet.

## Imaging low-mass planets within the habitable zones of nearby stars with ground-based mid-infrared imaging

Wagner, Kevin ; Ertel, Steve ; Stone, Jordan ; Leisenring, Jarron ; Apai, Dániel ; Kasper, Markus ; Absil, Olivier ; Close, Laird ; Defrère, Denis ; Guyon, Olivier ; Males, Jared

→ Submitted proceedings to SPIE Optical Engineering + Applications 2021, Techniques and Instrumentation for Detection of Exoplanets X

Giant exoplanets on 10-100 au orbits have been directly imaged around young stars. The peak of the thermal emission from these warm young planets is in the near-infrared ( $\sim 1\text{-}5$  microns), whereas mature, temperate exoplanets (i.e., those within their stars' habitable zones) radiate primarily in the mid-infrared (mid-IR:  $\sim 10$  microns). If the background noise in the mid-IR can be mitigated, then exoplanets with low masses—including rocky exoplanets—can potentially be imaged in very deep exposures. Here, we review the recent results of the Breakthrough Watch/ New Earths in the Alpha Centauri Region (NEAR) program on the Very Large Telescope (VLT) in Chile. NEAR pioneered a ground-based mid-IR observing approach designed to push the capabilities for exoplanet imaging with a specific focus on the closest stellar system, Alpha Centauri. NEAR combined several new optical technologies—including a mid-IR optimized coronagraph, adaptive optics system, and rapid chopping strategy to mitigate noise from the central star and thermal background within the habitable zone. We focus on the lessons of the VLT/NEAR campaign to improve future instrumentation—specifically on strategies to improve noise mitigation through chopping. We also present the design and commissioning of the Large Binocular Telescope's Exploratory Survey for Super-Earths Orbiting Nearby Stars (LESSONS), an experiment in the Northern hemisphere that is building on what was learned from NEAR to further push the sensitivity of mid-IR imaging. Finally, we briefly discuss some of the possibilities that mid-IR imaging will enable for exoplanet science.

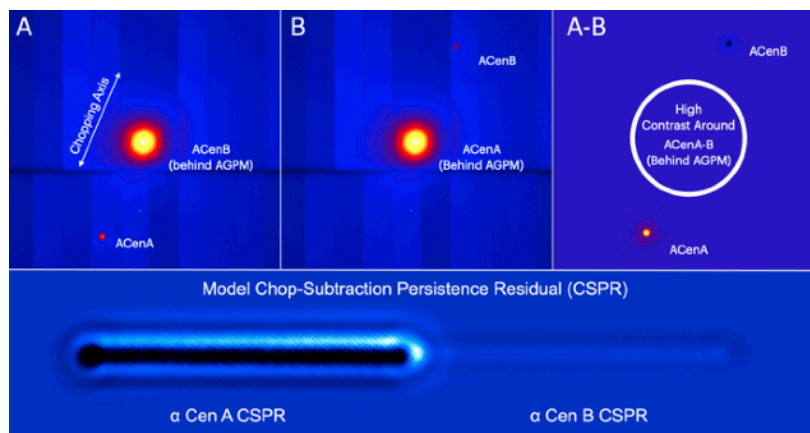


**Figure 1.** Top: an example of a chop-subtraction image pair from VLT/NEAR. Image B, following 0.05 sec after A, is subtracted to remove the detector bias, thermal background, AGPM glow, and excess low frequency noise (ELFN). Bottom: an example model of a chop-subtraction persistence residual (CSPR) of Centauri AB. This model was generated with an offset of  $\sim 2\%$  of a pixel, or  $\sim 1$  mas, of the star's position behind the coronagraph following each chop. The effects of the coronagraph, persistence non-linearity and temporal decay, and post-processing are not included in the model. The CSPR is too faint to be seen in the frames above, but is easily seen in longer integrations (see Fig. 2).

## A large sub-Neptune transiting the thick-disk M4V TOI-2406

Wells, R. D. et al.

→ Accepted for publication in *Astronomy and Astrophysics*

Large sub-Neptunes are uncommon around the coolest stars in the Galaxy and are rarer still around those that are metal-poor. However, owing to the large planet-to-star radius ratio, these planets are highly suitable for atmospheric study via transmission spectroscopy in the infrared, such as with JWST. Here we report the discovery and validation of a sub-Neptune orbiting the thick-disk, mid-M dwarf star TOI-2406. We first infer properties of the host star by analysing the star's near-infrared spectrum, spectral energy distribution, and Gaia parallax. We use multi-band photometry to confirm that the transit event is on-target and achromatic, and we statistically validate the TESS signal as a transiting exoplanet. We then determine physical properties of the planet through global transit modelling of the TESS and ground-based time-series data. We determine the host to be a metal-poor M4V star, located at a distance of 56 pc, with a sub-solar metallicity ( $[Fe/H] = -0.38 \pm 0.07$ ), and a member of the thick disk. The planet is a relatively large sub-Neptune for the M-dwarf planet population, with  $R_p = 2.94 \pm 0.17 R_\oplus$  and  $P = 3.077$  d, producing transits of 2% depth. We note the orbit has a non-zero eccentricity to  $3\sigma$ , prompting questions about the dynamical history of the system. This system is an interesting outcome of planet formation and presents a benchmark for large-planet formation around metal-poor, low-mass stars. The system warrants further study, in particular radial velocity follow-up to determine the planet mass and constrain possible bound companions. Furthermore, TOI-2406 b is a good target for future atmospheric study through transmission spectroscopy, particularly in the category of warm sub-Neptunes.

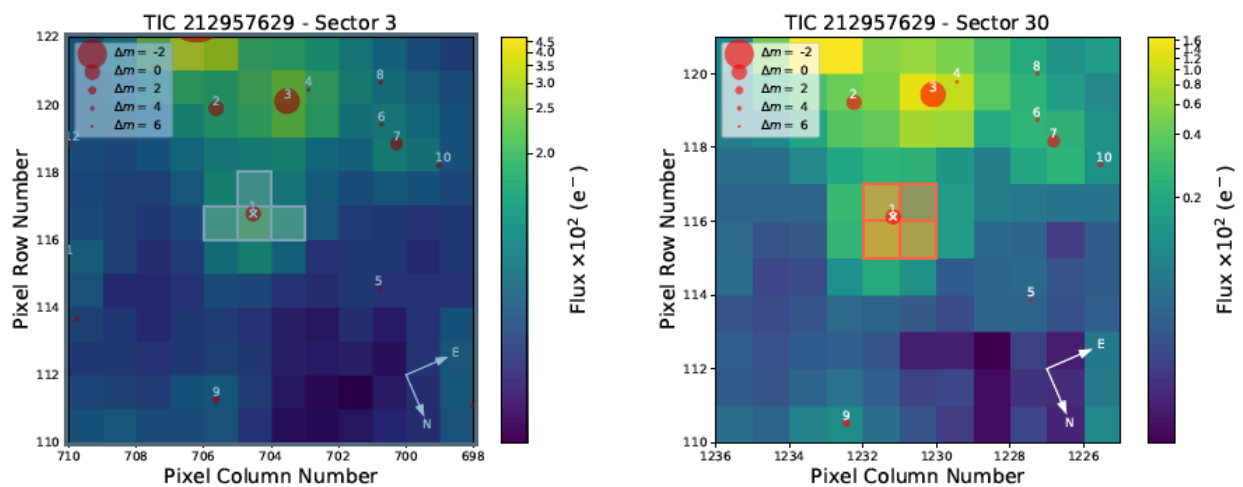


**Figure 1.** Target pixel file (TPF) images for TOI-2406, from TESS Sectors 3 (left) and 30 (right). The apertures used for light curve generation are over-plotted; sources identified in Gaia DR2 are also included, with symbols correlated to their brightness compared to the target. These images were produced using *tpfplotter* (Aller et al. 2020).

## ACCESS and LRG-BEASTS: A Precise New Optical Transmission Spectrum of the Ultrahot Jupiter WASP-103b

Kirk, James; Rackham, Benjamin V.; MacDonald, Ryan J.; López-Morales, Mercedes; Espinoza, Néstor; Lendl, Monika; Wilson, Jamie; Osip, David J.; Wheatley, Peter J.; Skillen, Ian; Apai, Dániel; Bixel, Alex; Gibson, Neale P.; Jordán, Andrés; Lewis, Nikole K.; Louden, Tom; McGruder, Chima D.; Nikolov, Nikolay; Rodler, Florian; Weaver, Ian C.

### → The Astronomical Journal, Volume 162, Issue 1

We present a new ground-based optical transmission spectrum of the ultrahot Jupiter WASP-103b ( $T_{\text{eq}} = 2484$  K). Our transmission spectrum is the result of combining five new transits from the ACCESS survey and two new transits from the LRG-BEASTS survey with a reanalysis of three archival Gemini/GMOS transits and one VLT/FORS2 transit. Our combined 11-transit transmission spectrum covers a wavelength range of 3900-9450 Å with a median uncertainty in the transit depth of 148 parts per million, which is less than one atmospheric scale height of the planet. In our retrieval analysis of WASP-103b's combined optical and infrared transmission spectrum, we find strong evidence for unocculted bright regions ( $4.3\sigma$ ) and weak evidence for H<sub>2</sub>O ( $1.9\sigma$ ), HCN

( $1.7\sigma$ ), and TiO ( $2.1\sigma$ ), which could be responsible for WASP-103b's observed temperature inversion. Our optical transmission spectrum shows significant structure that is in excellent agreement with the extensively studied ultrahot Jupiter WASP-121b, for which the presence of VO has been inferred. For WASP-103b, we find that VO can only provide a reasonable fit to the data if its abundance is implausibly high and we do not account for stellar activity. Our results highlight the precision that can be achieved by ground-based observations and the impacts that stellar activity from F-type stars can have on the interpretation of exoplanet transmission spectra.

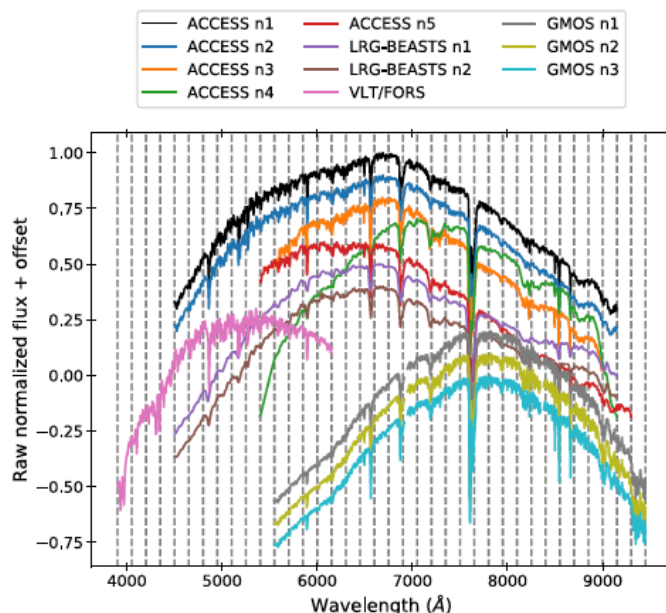


**Figure 1.** WASP-103's nightly mean-averaged spectra as observed on each of the 11 nights used in our analysis, grouped by instrument and with an offset applied for clarity. The different spectral shapes are a result of the different instrument throughputs. The dashed vertical lines indicate the edges of the thirty-seven 150 Å-wide bins we used to generate the spectroscopic transit light curves.

## EDEN: Flare Activity of the Nearby Exoplanet-hosting M Dwarf Wolf 359 Based on K2 and EDEN Light Curves

Lin, Chia-Lung; Chen, Wen-Ping; Ip, Wing-Huen; Apai, Dániel; Bixel, Alex; Boyle, Richard; Chavez, Jose Perez; Espinoza, Nestor; Gibbs, Aidan; Gabor, Paul ; Henning, Thomas; Mancini, Luigi; Rackham, Benjamin V.; Schlecker, Martin; Dietrich, Jeremy; Socia, Quentin Jay; Keppler, Miriam; Bhandare, Asmita; Häberle, Maximilian

### → The Astronomical Journal, Volume 162, Issue 1

We report the flare activity of Wolf 359, the fifth closest star to the Sun and a candidate exoplanet-hosting M dwarf. The star was a target of the Kepler/K2 mission and was observed by the EDEN project, a global network of 1-2 m class telescopes for detection and characterization of rocky exoplanets in the habitable zones of late-M dwarfs within 50 light year from the solar system. In the combination of the archived K2 data and our EDEN observations, a total of 872 flares have been detected, 861 with the K2 (860 in the short-cadence and 18 in the long-cadence data, with 17 long-cadence events having short-cadence counterparts) and 11 with EDEN. Wolf 359 has relatively strong flare activity even among flaring M dwarfs, in terms of the flare activity indicator (FA) defined as the integrated flare energy relative to the total stellar bolometric energy, where  $FA = \sum E_f / \int L_{bol} dt \sim 8.93 \times 10^{-5}$  for the long-cadence flares, whereas for K2 short cadence and EDEN flares, the FA values are somewhat larger,  $FA \approx 6.67 \times 10^{-4}$  and  $FA \approx 5.25 \times 10^{-4}$ , respectively. Such a level of activity, in accordance with the rotation period ( $P_{rot}$ ), suggests the star to be in the saturation phase. The size of the starspots is estimated to be at least  $1.87\% \pm 0.59\%$  of the projected disk area of Wolf 359. We find no correlation of FA with the stellar rotational phase. Our

analysis indicates a flare frequency distribution in a power-law form of  $dN/dE \propto E^{-\alpha}$  with  $\alpha = 2.13 \pm 0.14$ , equivalent to an occurrence rate of flares  $E_f \geq 1031$  erg about once per day and of superflares with  $E_f \geq 1033$  erg approximately 10 times per year. These superflares may impact the habitability of system in multiple ways, the details of which are topics for future investigations.

Target ID: 201885041, Cadence: 4348901

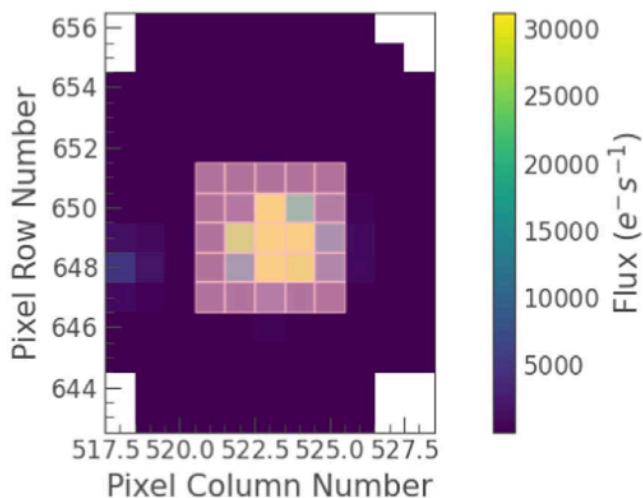


**Figure 2.** An arbitrary cadence of K2 SC target pixel data of Wolf 359. The area covered by transparent white is the aperture used to extract the light curve.

## Bioverse: A Simulation Framework to Assess the Statistical Power of Future Biosignature Surveys

Bixel, Alex; Apai, Daniel

→ [The Astronomical Journal, Volume 161, Issue 5](#)

Next-generation space observatories will conduct the first systematic surveys of terrestrial exoplanet atmospheres and search for evidence of life beyond Earth. While in-depth observations of the nearest habitable worlds may yield enticing results, there are fundamental questions about planetary habitability and evolution that can only be answered through population-level studies of dozens to hundreds of terrestrial planets. To determine the requirements for next-generation observatories to address these questions, we have developed Bioverse. Bioverse combines existing knowledge of exoplanet statistics with a survey simulation and hypothesis testing framework to determine whether proposed space-based direct imaging and transit-spectroscopy surveys will be capable of detecting various hypothetical statistical relationships between the properties of terrestrial exoplanets. Following a description of the code, we apply Bioverse to determine whether an ambitious direct imaging or transit survey would be able to determine the extent of the circumstellar habitable zone and study the evolution of Earth-like planets. Given

recent evidence that Earth-sized habitable zone planets are likely much rarer than previously believed, we find that space missions with large search volumes will be necessary to study the population of terrestrial and habitable worlds. Moving forward, Bioverse provides a methodology for performing trade studies of future observatory concepts to maximize their ability to address population-level questions, including and beyond the specific examples explored here.

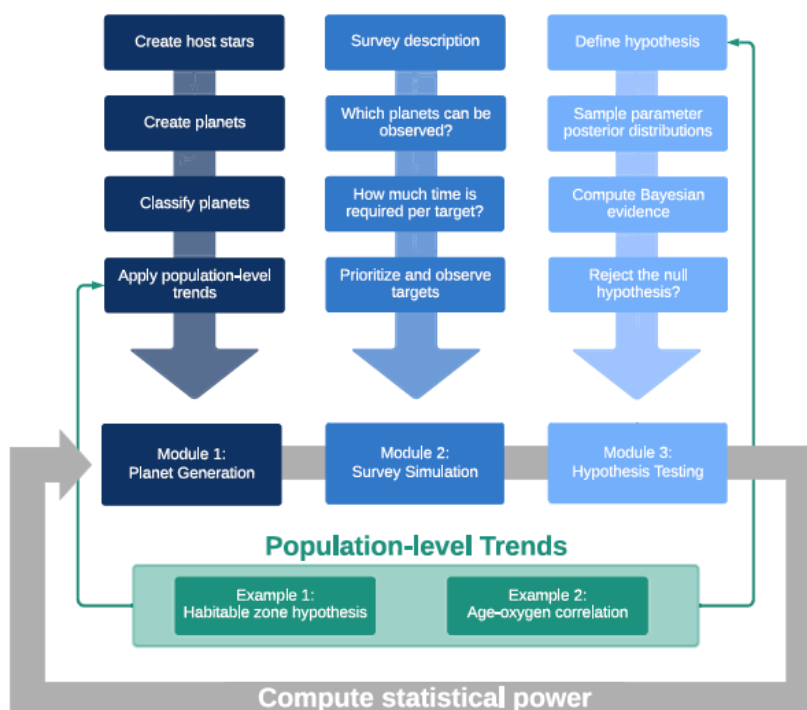


**Figure 1.** High-level outline of the Bioverse code. In this paper, we apply Bioverse to assess the detectability of two hypothetical population-level trends (green) with next-generation survey telescopes. These relationships are injected into the simulated planet population by the first module, then tested as statistical hypotheses by the third module.